UC San Diego
UC San Diego Previously Published Works

Title

An Assessment of Density-Based Finescale Methods for Estimating Diapycnal Diffusivity in the Southern Ocean

Permalink

https://escholarship.org/uc/item/3ns2x13q

Journal

Journal of Atmospheric and Oceanic Technology, 30(11)

ISSN

0739-0572

Authors

Frants, Marina
Damerell, Gillian M
Gille, Sarah T
et al.

Publication Date

2013-11-01

DOI

10.1175/jtech-d-12-00241.1

Peer reviewed

An Assessment of Density-Based Finescale Methods for Estimating Diapycnal Diffusivity in the Southern Ocean

Marina Frants*

Scripps Institution of Oceanography, La Jolla, California

Gillian M. Damerell

School of Environmental Sciences, University of East Anglia, Norwich, United Kingdom

Sarah T. Gille

Scripps Institution of Oceanography, La Jolla, California

Karen J. Heywood

School of Environmental Sciences, University of East Anglia, Norwich, United Kingdom

Jennifer MacKinnon and Janet Sprintall

Scripps Institution of Oceanography, La Jolla, California

(Manuscript received 16 November 2012, in final form 7 August 2013)

ABSTRACT

Finescale estimates of diapycnal diffusivity κ are computed from CTD and expendable CTD (XCTD) data sampled in Drake Passage and in the eastern Pacific sector of the Southern Ocean and are compared against microstructure measurements from the same times and locations. The microstructure data show vertical diffusivities that are one-third to one-fifth as large over the smooth abyssal plain in the southeastern Pacific as they are in Drake Passage, where diffusivities are thought to be enhanced by the flow of the Antarctic Circumpolar Current over rough topography. Finescale methods based on vertical strain estimates are successful at capturing the spatial variability between the low-mixing regime in the southeastern Pacific and the high-mixing regime of Drake Passage. Thorpe-scale estimates for the same dataset fail to capture the differences between Drake Passage and eastern Pacific estimates. XCTD profiles have lower vertical resolution and higher noise levels after filtering than CTD profiles, resulting in XCTD κ estimates that are, on average, an order of magnitude higher than CTD estimates. Overall, microstructure diffusivity estimates are better matched by strain-based estimates than by estimates based on Thorpe scales, and CTD data appear to perform better than XCTD data. However, even the CTD-based strain diffusivity estimates can differ from microstructure diffusivities by nearly an order of magnitude, suggesting that density-based fine-structure methods of estimating mixing from CTD or XCTD data have real limitations in low-stratification regimes such as the Southern Ocean.

1. Introduction

Diapycnal turbulent mixing is a dominant factor in controlling the stratification and energy budget of the global ocean, as well as vertical fluxes of freshwater, nutrients, and dissolved tracers (e.g., Munk and Wunsch 1998). In the upper ocean, it drives the heat and gas exchanges between the ocean and the atmosphere, influencing the ocean's role in regulating global climate. Observations have revealed a high degree of spatial variability in diapycnal diffusivity κ, with typical background diffusivities of $10^{-5}\,\mathrm{m^2\,s^{-1}}$ in the top 1000 m of the water column, and regions of intense mixing, where κ can be as high as $10^{-3}\,\mathrm{m^2\,s^{-1}}$ (Gregg 1987; Toole et al. 1994). Spatial variations of diapycnal mixing have

* Current affiliation: University of New South Wales, Sydney, New South Wales, Australia.

Corresponding author address: Marina Frants, University of New South Wales, Sydney, NSW 2052, Australia.
E-mail: m.frants@unsw.edu.au

significant implications for ocean circulation and climate modeling (e.g., Simmons et al. 2004; Palmer et al. 2007; Nikurashin and Legg 2011), and numerical models run with patchy mixing have substantially different upwelling patterns than models with uniform mixing (e.g., Jochum 2009). Thus, characterizing the spatial patterns of vertical diffusivities in the ocean has emerged as a priority research topic (MacKinnon et al. 2010).

Vertical diffusivities have typically been inferred from tracer release experiments, which measure the integrated effect of vertical diffusivity over many months (e.g., Ledwell et al. 2000, 2011), or from microstructure profiler measurements, which are specifically designed to resolve the small vertical length scales thought to be responsible for diapycnal mixing in the ocean (e.g., Toole et al. 1994; Polzin et al. 1995; St. Laurent et al. 2012). However, the availability of these measurements is limited because of cost, the need for trained personnel, and the difficulty of deploying the instruments in rough weather conditions. As a result, a number of alternative methods of estimating κ from finescale measurements have been developed, including methods based on detecting static instabilities in otherwise stably stratified density profiles (Thorpe 1977; Dillon 1982) and on parameterizations of internal wave shear and strain variances (Kunze 2003). Such finescale approaches have been applied to a wide range of observations made with velocity profiles from lowered acoustic Doppler current profilers (LADCP) (e.g., Kunze et al. 2006; Naveira Garabato et al. 2004) or with density profiles from CTDs (e.g., Sloyan, 2005; Kunze et al. 2006; Gargett and Garner, 2008; Sloyan et al. 2010), expendable CTDs (XCTDs) (e.g., Thompson et al. 2007; Sloyan et al. 2010), and Argo floats (Wu et al. 2011; Whalen et al. 2012). These estimates involve a number of approximations, the accuracy of which has not been fully determined. Comparisons between the Thorpe-scale method and microstructure estimates showed good agreement in regions of high stratification and favorable sampling conditions, such as low winds or a stable platform to reduce ship motion (Seim and Gregg 1994; Klymak et al. 2008; Ferron et al. 1998). However, ship motion effects and low-stratification conditions can affect the accuracy of finescale methods in extreme environments such as the Southern Ocean.

Because finescale methods offer the promise of inexpensive global maps of vertical diffusivity, there is a strong impetus to apply them to the existing archive of hydrographic data. Density profiles are of particular interest because there is a long historical archive of density data, and because the growing database of Argo profiles provides approximately 3000 new density profiles every 10 days (Roemmich et al. 2009). The objective of this study is to provide an assessment of finescale κ derived from CTD and XCTD density profiles in direct comparison with concurrent microstructure measurements collected as part of the Diapycnal and Isopycnal Mixing Experiment in the Southern Ocean (DIMES).

DIMES was conceived to measure both diapycnal mixing and isopycnal stirring over the comparatively smooth topography of the southeastern Pacific (upstream of Drake Passage) and through the rough topography of Drake Passage and the Scotia Sea, where internal wave activity was expected to generate enhanced vertical mixing (Gille et al. 2007, 2012; St. Laurent et al. 2012). The diapycnal mixing component of the project included purposeful tracer release as well as microstructure measurements. The finescale component carried out an extensive measurement campaign that included LADCP, XCTD, and CTD sampling that was intended to facilitate an assessment of finescale methods. Results from the LADCP data will be reported separately (A. Thurnherr 2012, personal communication), and this study focuses specifically on density profile data.

DIMES measurements in the southeastern Pacific centered about the tracer release isopycnal, which had an average depth of 1500 m, showed κ to be (0.75 ± 0.07) $\times$ 10^{-5} m^2 s^{-1} on the basis of microstructure measurements taken during the summer, and (1.3 ± 0.2) $\times$ 10^{-5} m^2 s^{-1} on the basis of tracer diffusion averaged over a year (Ledwell et al. 2011). In Drake Passage, St. Laurent et al. (2012) reported an order of magnitude more mixing, with mean values of κ found to be 1.3×10^{-4} m^2 s^{-1}. Similarly, in a separate field program in the Indian Ocean sector of the Southern Ocean, Waterman et al. (2013) also found a strong contrast between regions of smooth seafloor and rough topography, with κ values averaging 6.9×10^{-5} m^2 s^{-1} over most of the region but reaching a maximum of 3.4×10^{-3} m^2 s^{-1} near the steep terrain of the Kerguelen Plateau.

Previous finescale estimates in the Southern Ocean have indicated enhanced mixing over rough bathymetry (e.g., Sloyan 2005) and have indicated diffusivities in Drake Passage, with κ ranging from $O(10^{-4})$ to $O(10^{-3})$ m^2 s^{-1} (Naveira Garabato et al. 2004; Thompson et al. 2007), somewhat higher than inferred from the DIMES microstructure or tracer measurements. More recently, Sheen et al. (2013) found middepth turbulent dissipation rates increasing by an order of magnitude between the southeastern Pacific and the Scotia Sea. While finescale estimates might be predicted to overestimate the magnitude of turbulent diapycnal mixing in the ocean due to the effects of instrument noise on density profiles and spectra, at a minimum we expect that a successful diapycnal diffusivity estimate should be able to capture
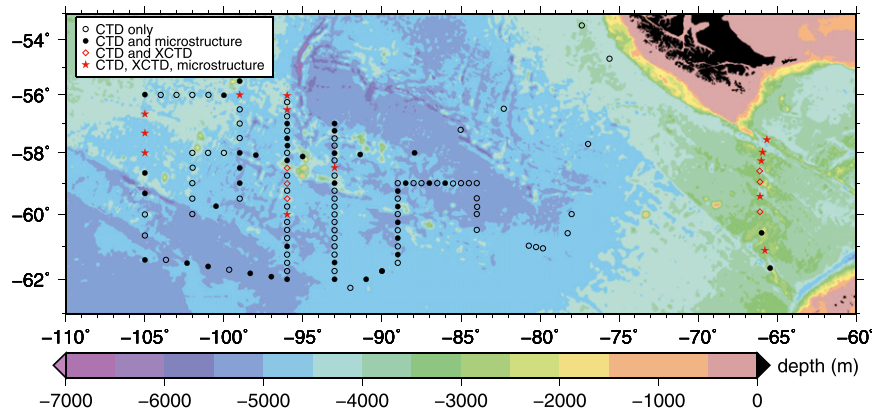
FIG. 1. Locations of CTD stations, XCTD stations, and microstructure profiler stations sampled during the DIMES US2 cruise in summer 2010. Here red stars indicate stations for which concurrent microstructure, CTD, and XCTD casts are available; red open circles indicate concurrent CTD and XCTD casts; black filled dots indicate concurrent CTD and microstructure; and black open circles indicate only CTD data.

the differences in the magnitude of the diffusivities between the abyssal plain in the southeastern Pacific and the rough topography Drake Passage (Ledwell et al. 2011; St. Laurent et al. 2012; Sheen et al. 2013).

To compute finescale diapycnal diffusivity from density profiles, we consider the Thorpe-scale method and the vertical strain method. Both methods depend only on density profiles and can therefore be applied when neither microstructure data nor LADCP measurements are available. Thus, the Thorpe-scale and strain methods have the potential to provide mixing estimates over a wide spatial and temporal range, provided the data are of sufficient quality and vertical resolution. The goal of our analysis is first to determine whether either method used with CTD and XCTD profiles can replicate the basic geographic contrast between high and low κ reported in the microstructure data. Our second goal is to provide guidance about the accuracy and performance of finescale methods in the low-stratification environment of the Southern Ocean.

2. Data and methods

a. Data

Finescale and microstructure data used for this study were collected during the January and February 2010 DIMES cruise aboard Research Vessel (R/V) *Thomas G. Thompson*. The survey area covered a region between the polar front and the Southern Antarctic Circumpolar Current Front in the southeastern Pacific, as well as a transect across Drake Passage near 65°W. A total of 137 usable CTD profiles, using two sets of Sea-Bird Electronics SBE 9*plus* sensors, and 19 usable

XCTD profiles were obtained at locations shown in Fig. 1. Both finescale instruments were deployed concurrently with each other and with one of the microstructure profilers where possible, specifically to facilitate comparing finescale mixing estimates against microstructure measurements. Four of the CTD casts were deployed to a target depth of 5000 m, and the rest were deployed to 2000 m or to 10 m above the bottom, whichever is shallower. However, XCTD probes sample to a maximum depth of 1100 m. For this analysis, we only use the data from the top 1000 m, both to facilitate comparisons with the XCTD and because this depth range is sampled most extensively by the Argo program and by glider campaigns. Therefore, evaluation of finescale performance in the top 1000 m is a prerequisite for determining what we can learn from routine density profiles.

Microstructure measurements of temperature, conductivity, and velocity shear were sampled with the High Resolution Profiler 2 (HRP2) provided by Woods Hole Oceanographic Institution and the Deep Microstructure Profiler (DMP), provided by Rockland Scientific International, Inc. A total of 40 usable profiles were obtained with HRP2 and 22 profiles with the DMP. Ledwell et al. (2011) provide detailed information about the instruments and the sampling methodology. The profiles were averaged into 0.5-m bins for the HRP2 and into 1-m bins for the DMP. Figure 1 indicates the station locations where microstructure profiles coincide with XCTD or CTD profiles. A total of 13 stations produced usable density profiles from all three instruments. The locations of these stations are shown as red stars in Fig. 1.

In optimal conditions, we would compare the microstructure κ estimates against separate finescale κ estimates

derived from HRP2/DMP, CTD, and XCTD density profiles. However, the HRP2 microstructure profiler suffered from salinity spiking issues, for which a correction has not yet been determined (L. C. St. Laurent 2012, personal communication). We considered using temperature profiles below the subsurface temperature maximum in order to evaluate finescale diffusivity, following an approach tested by Thompson et al. (2007). However, temperature and density spectra differ substantially (not shown), implying that even below the temperature maximum, salinity and temperature variations typically compensate each other, so that temperature alone is not representative of the density field. Thus, the finescale results presented here are based on CTD and XCTD profiles only, and these are compared with velocity shear–based microstructure estimates of κ from the HRP2 and DMP probes.

b. Methods

1) DATA PREPROCESSING AND NOISE ESTIMATION

Both of the finescale parameterization methods used in our analysis require a clear understanding of the noise characteristics of the data, as well as sufficient vertical resolution to resolve the turbulence. The raw data must be carefully processed in order to minimize the effects of instrument noise and measurement errors (Gargett and Garner 2008; Gille et al. 2009; Uchida et al. 2011).

The temperature and conductivity sensors on the 9*plus* CTD sample at 24 Hz. At typical winch speeds, this results in a vertical spatial resolution of approximately 3 cm. However, the resolution will vary with changes in winch speed. CTDs are also subject to ship roll, which can create pressure reversals in the measured profiles. XCTDs record measurements at 25 Hz, equivalent to approximately 14-cm vertical resolution. They fall freely through the water column and are not affected by ship motion. However, they are not intended to be high-precision instruments.

Gille et al. (2009) found that almost all XCTDs exhibit anomalous spectral spikes at the 5- and 10-Hz sampling frequencies in both the temperature and the conductivity spectra. They advocated low-pass filtering the data to remove energy at frequencies of 5 Hz or greater. Accordingly, for this study we designed a least squares low-pass filter where the spectral energy tapers from 1 to 0 in the frequency range between 22% and 34% of the 12.5-Hz Nyquist frequency. Filter widths ranging from 1 to 10 m were considered, and a 3-m filter, corresponding to 21 data points at typical XCTD resolution, was found to perform best in reducing the spectral spiking. This filter was used in addition to the low-pass Hamming filter with a 19-scan window as suggested by
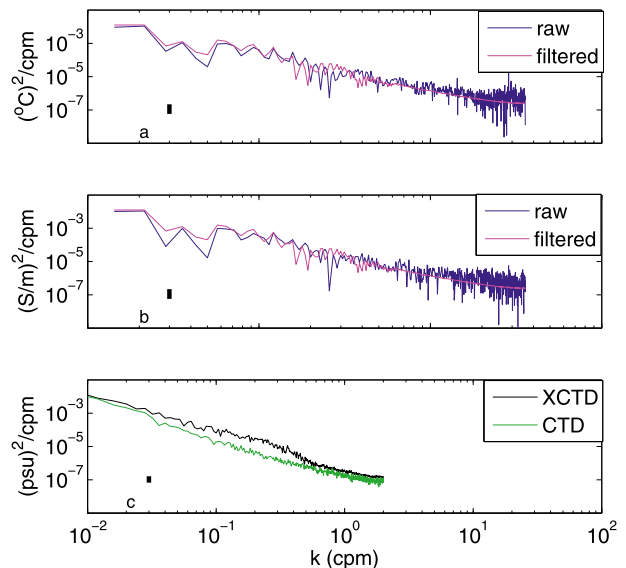

FIG. 2. Comparison of raw and filtered spectra of (a) temperature and (b) conductivity for XCTD profiles sampled in Drake Passage during the 2010 DIMES survey; and (c) comparison of filtered, binned, and time lag–corrected salinity spectra for CTD and XCTD profiles sampled in Drake Passage during the 2010 DIMES survey. Error bars represent 95% confidence intervals, computed based on the χ^2 cumulative distribution of the spectra (Bendat and Piersol 2000). For each comparison, spectra from all available Drake Passage casts were calculated from detrended 1000-point profile segments centered on 600-m depth and then averaged together. [Vertical resolution differs for the processed data used in (c), compared with the data used in (a) and (b), and this accounts for a difference in the range of wavenumbers considered.]

Uchida et al. (2011). Filtered and unfiltered spectra for the DIMES profiles sampled in Drake Passage are shown in Figs. 2a,b.

Both CTDs and XCTDs are subject to salinity spiking caused by the differing time responses of the temperature and conductivity sensors (Johnson et al. 2007; Gargett and Garner 2008). To minimize the effects of this spiking for both instruments, we utilized an iterative procedure similar to the approach used by Johnson et al. (2007) to estimate the lag between sensor pairs by minimizing the cross-spectral phase and maximizing the squared coherence between temperature and conductivity (R. Todd 2012, personal communication). After correcting for the thermal lag, pressure reversals caused by ship roll were removed from the CTD profiles (Gargett and Garner 2008), and salinity was computed from the filtered and lag-corrected data. Finally, all data were linearly interpolated to 0.25-m depth intervals. The resulting wavenumber spectra of salinity, which showed the largest differences between CTD and XCTD after processing, are shown in Fig. 2c.

Even in cases without pressure reversals, ship roll may also create measurement errors in CTD data caused by

the turbulent wake generated when the rosette's descent or ascent rate abruptly changes. To correct for this wake effect, we performed a test run with the raw data preprocessed to remove all scans where the descent rate had slowed to less than $0.2\,\mathrm{m\,s^{-1}}$. We found that this correction had no effect on the diffusivity estimates, and it was not included in our final analysis.

Thorpe-scale estimates of diffusivity are based on the identification of overturns in density profiles. Since instrument noise can produce false overturns, an estimate of such noise is necessary for overturn validation. The raw XCTD profiles in our dataset show uniformly sized, discrete fluctuations of $\pm0.01°\mathrm{C}$ for temperature and $\pm0.02\,\mathrm{S\,m^{-1}}$ for conductivity, implying corresponding measurement uncertainties of $0.005°\mathrm{C}$ and $0.01\,\mathrm{S\,m^{-1}}$. Propagating these uncertainties to the salinity and density calculations result in a density uncertainty of approximately $0.012\,\mathrm{kg\,m^{-3}}$. Filtering the data with the 21- and 19-point filters as described above reduces the density uncertainty to approximately $0.005\,\mathrm{kg\,m^{-3}}$.

The raw CTD data do not exhibit the uniform fluctuations seen in the XCTD data. To estimate the noise in our processed CTD density profiles, we followed the procedure described by Gargett and Garner (2008) and examined individual profiles, defining the noise level for each profile to be the standard deviation of detrended density values within a 10-m layer where density is well mixed. Based on this criterion, the noise level in the CTD density profiles was approximately $4 \times 10^{-4}\,\mathrm{kg\,m^{-3}}$.

Based on our noise estimates, we can follow the methods used by Gargett and Garner (2008) to predict a minimum size for resolvable density overturns in our data. At depths between 600 and 1000 m for typical lowstratification profiles in our study region, density changes of $0.005\,\mathrm{kg\,m^{-3}}$ occur over depth changes of 5–7 m, and changes of $4 \times 10^{-4}\,\mathrm{kg\,m^{-3}}$ occur over 0.5–1.5 m. For our validation criteria, we require a minimum of three data points in each overturn, leading to a cutoff of 15–21 m for XCTD overturns, matching our upper limit based on the raw data. For the CTD, the cutoff is between 1.5 and 4.5 m. Therefore, to reduce the number of false overturns, we discarded all XCTD overturns of less than 20 m and all CTD overturns of less than 4 m, or having a density difference of less than twice the instrument noise. This criterion resulted in 69% of all XCTD overturns and 76% of all CTD overturns being rejected as too small. To evaluate the effect of our choice of minimum overturn size on the diffusivity estimates, we also performed our analysis of the CTD data using a minimum overturn of 20 m to match the XCTD analysis. The resulting κ estimates were within one standard error of the estimates computed with a 4-m minimum

overturn size. The result suggests that overturns larger than 20 m have a disproportionate effect on κ. Large overturns are more likely to include noise-generated density spikes that can lead to overestimation of Thorpe scales and thus to overestimation of κ.

2) THORPE-SCALE ANALYSIS AND ADDITIONAL OVERTURN VALIDATION

Thorpe-scale analysis (Thorpe 1977) provides a method for estimating small-scale mixing rates from temperature and salinity data in places where direct microstructure measurements are not available. The goal of the analysis is to determine kinetic energy dissipation rate ϵ and diapycnal eddy diffusivity κ. The value of ϵ is related to the Ozmidov-scale L_O (Ozmidov 1965) by

$$\epsilon = L_O^2 N^3, \tag{1}$$

where N is the background buoyancy frequency.

The Thorpe-scale L_T is obtained by reordering a vertical profile that contains density overturns in order to create a stably stratified profile. For a given overturn, it is defined as

$$L_T \equiv \sqrt{\langle d'^2 \rangle}, \tag{2}$$

where Thorpe displacement d' is the displacement of every reordered point from its original position in the profile.

Comparisons between L_O and L_T suggest a linear relationship between the two scales (Dillon 1982; Crawford 1986). Dillon (1982) found the coefficient to be $L_O = (0.8 \pm 0.4)L_T$. Substituting this relationship into (1) allows us to compute the energy dissipation for each individual overturn as

$$\epsilon_i = 0.64 L_{Ti}^2 \langle N \rangle_i^3, \tag{3}$$

where i refers to the ith overturn and $\langle N \rangle_i$ is the depth-averaged buoyancy frequency over the overturn region.

Diapycnal eddy diffusivity can be computed from ϵ as

$$\kappa = \Gamma \epsilon N^{-2}, \tag{4}$$

where Γ is the mixing efficiency. Here we follow common convention (e.g., Thompson et al. 2007) and assume $\Gamma = 0.2$.

Galbraith and Kelley (1996) proposed a water mass test for processed data, designed to reduce the number of false overturns caused by the mismatch in sensor

response times, particularly in regions where temperature and conductivity vary rapidly with depth. The test is based on performing linear least squares fits to temperature and salinity within each overturn and computing the root-mean-square (RMS) of the differences between the fitted lines and the data. The results are then normalized by the RMS difference between the sorted and the unsorted density values within the same overturn to produce the quantities ζ_t for temperature and ζ_s for salinity. The quantity $\zeta = \max(\zeta_s, \zeta_t)$ can then be used as a measure of the tightness of the T–S relationship within the overturn. Galbraith and Kelley (1996) proposed $\zeta < 0.5$ as the threshold for overturn validation. However, Martin and Rudnick (2007) and Thompson et al. (2007) have found that a less stringent criterion of $\zeta < 1$ is sufficient, and we accordingly adopt the criterion of $\zeta < 1$ for our own analysis.

As a final step in reducing noise-related false overturns, we followed Gargett and Garner's (2008) method of creating an intermediate density profile in which a constant density is maintained until a density change greater than a specified threshold value occurs between two successive data points. Potential overturns in the intermediate profiles were then evaluated based on both the Galbraith and Kelley (1996) criterion and the overturn ratio criterion as suggested by Gargett and Garner (2008):

$$R_0 = \min(L^+/L, L^-/L), \tag{5}$$

where L is the length of an overturn, L^+ is the length of that portion of L where the Thorpe displacements are positive, and L^- is the length of the portion where the displacements are negative. Values of $R_0 < 0.2$ implied that the prospective overturn was caused by a single density spike that might have been due to instrument noise, and overturns with these values were rejected.

For both CTD and XCTD data, the κ estimates for each cast were averaged into 100-m depth bins, and error bars were calculated as one standard error based on one standard deviation of the values averaged in each bin.

3) VERTICAL STRAIN ANALYSIS

A second method of estimating κ derives from examining the energy spectra of vertical strain in the internal wave field. In the stratified ocean, nonlinear interactions among internal waves transfer energy from higher wavelengths to increasingly unstable, smaller wavelengths, eventually leading to turbulence. Comparison of various wave-dissipation models (Wijesekera et al. 1993) has shown that κ estimates that are in good agreement with observational data can be obtained by

comparing the spectrum of the internal-wave-field strain rates with a model Garrett and Munk (GM) spectrum proposed by Garrett and Munk (1975).

Strain variance level $\langle \xi_z^2 \rangle$ is computed by integrating the Fourier-transformed spectral representation ϕ_λ of the buoyancy frequency to determine the maximum wavenumber $k_{\max}$ such that

$$\langle \xi_z^2 \rangle = \int_{k_{\min}}^{k_{\max}} \phi_\lambda \, dk = 0.2. \tag{6}$$

The minimum wavenumber $k_{\min} = 0.01 \, \mathrm{m}^{-1}$ was selected following recommendations made by Kunze et al. (2006), who found that strain spectra at wavelengths greater than 100 m are frequently contaminated by background stratification. Like Thompson et al. (2007), we found that varying the constant 0.2 in (6) had no significant effect on the spatial distribution or magnitude of the mixing.

The strain variance level for the GM spectrum is computed for the same wavenumber range as

$$\langle \xi_z^2 \rangle_{\mathrm{GM}} = \frac{\pi E_0 b j_*}{2} \int_{k_{\min}}^{k_{\max}} \frac{k^2}{(k + k_*)^2} \, dk, \tag{7}$$

where E_0 is the dimensionless energy level; b is the scale thermocline depth; j_* is the reference mode number; and $2\pi k_*$ is the reference wavenumber, defined as $0.0073(N/N_0)$. Following Gregg and Kunze (1991), we set these parameters to be $E_0 = 6.3 \times 10^{-5}$, $b = 1300 \, \mathrm{m}$, $j_* = 3$, and $N_0 = 0.005 \, 24 \, \mathrm{s}^{-1}$.

Strain-derived vertical diffusivity κ^ϕ can be calculated from (6) and (7) as

$$\kappa^\phi = \kappa_0 \frac{\langle \xi_z^2 \rangle^2}{\langle \xi_z^2 \rangle_{\mathrm{GM}}^2} H(R_\omega) J(f, N), \tag{8}$$

with $\kappa_0 = 0.05 \times 10^{-4} \, \mathrm{m}^2 \, \mathrm{s}^{-1}$.

In (8) H and J are empirical functions that account for the effect of latitude on the internal wave field. The function H is given as

$$H(R_\omega) = \frac{3R_\omega(R_\omega + 1)}{4(R_{\omega\mathrm{GM}}^2)} \sqrt{\frac{2}{R_\omega - 1}}, \tag{9}$$

where $R_\omega = \langle V_z^2 \rangle / (N^2 \langle \xi_z^2 \rangle)$ is the shear/strain ratio, with V_z being the vertical derivative of horizontal velocity. For our calculations, we followed Kunze et al. (2006) and Thompson et al. (2007) and $R_{\omega\mathrm{GM}} = 3$, while R_ω was set to 7 based on LADCP measurements from our study region (A. Thurnherr 2012, personal communication).
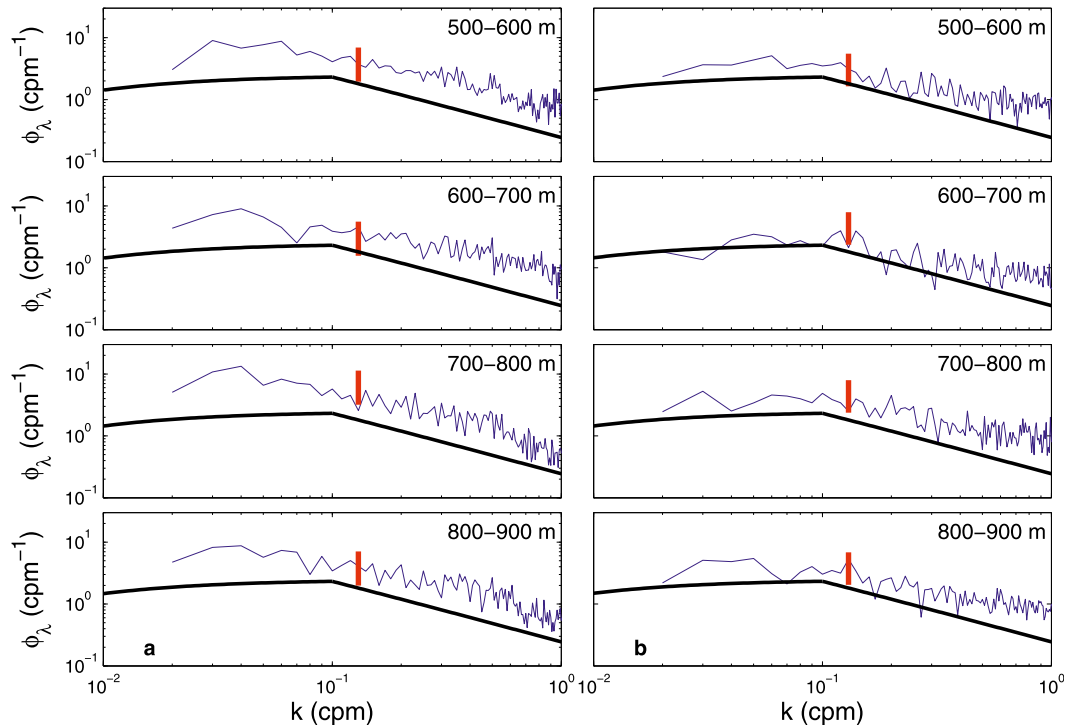
FIG. 3. Comparison between averaged vertical strain spectra of Fourier-transformed buoyancy frequency (blue) for the (a) XCTD and (b) CTD stations in Drake Passage, and the GM model spectrum (thick black line). Vertical red lines indicate error bars representing the 95% confidence interval, computed based on the χ^2 cumulative distribution of the spectra (Bendat and Piersol 2000).

The use of a spatially constant value for R_ω introduces a possible bias in our results, as Waterman et al. (2013) and Sheen et al. (2013) have found significant variation in shear/strain ratios in our study region. However, setting R_ω to values ranging from 5 to 10 produced results (not shown) that were consistent within error bars with our final estimates.

Function J is given as

$$J(f, N) = \frac{f \cosh^{-1}(N/f)}{f_{30} \cosh^{-1}(N_0/f_{30})}, \tag{10}$$

where $f_{30} = 7.29 \times 10^{-5}\,\mathrm{s}^{-1}$ is the Coriolis frequency at 30° latitude, and N_0 is the reference buoyancy frequency as defined for (7).

Thompson et al. (2007) used (8)–(10) to calculate spectra based on both buoyancy frequency and potential density profiles across Drake Passage, and found that both quantities produced spectra of similar amplitudes, with differences of less than 15%. Both spectra also showed the same spatial pattern of κ values across the passage. For our analysis, we used buoyancy frequency spectra, computed using the method described by Kunze (2003) and followed by Thompson et al. (2007).

To compare the vertical strain diffusivities for CTD and XCTD data, we computed κ^ϕ estimates for the CTD and XCTD sections sampled in the southeastern Pacific sector and in Drake Passage during the DIMES survey. For every buoyancy frequency profile in the transect, we divided the data into 100-m depth bins, discarding the top 200 m to eliminate the mixed layer and the effects of the ship's draft near the surface. We normalized the data in each bin by the average buoyancy frequency for that bin and then subtracted a linear trend. The Fourier transforms of the normalized and detrended data were then averaged within each bin to obtain the spectral estimate. The resulting spectra for the XCTD and CTD, as well as the GM spectrum, are shown in Fig. 3 for the middepth bins for all the stations in the Drake Passage transect.

3. Results and discussion

The diffusivity estimates produced by both Thorpe-scale and vertical strain methods depend on the noise inherent in the available density profiles. We compare values of κ obtained from two sets of DIMES stations in which CTDs and XCTDs were deployed concurrently.

One set consisted of stations located in the eastern Pacific sector of the Southern Ocean west of 70°W, while the other was sampled along a transect in Drake Passage near 65°W, as indicated in Fig. 1.

a. Thorpe-scale method

Thorpe-scale κ estimates are shown in Figs. 4a,b for XCTD (blue) and CTD (green). Microstructure estimates (magenta) are also included for comparison. For each depth bin, the mean diffusivity estimates plotted here are determined by averaging results from the stations marked with red stars in Fig. 1. To leading order, the microstructure, XCTD-, and CTD-derived diffusivities are lognormally distributed, and the one standard error uncertainties plotted here are computed from the standard deviation of log(κ). Davis (1996) found that the variance dissipation of a tracer (χ) has a "cut of lognormal" distribution, which increases for smaller values and reaches a maximum at zero, rather than a true lognormal distribution. However, it is not clear that ϵ or κ have the same distribution as χ. Given the limited size of our dataset and the relatively uniform background stratification in our sampling region, we concluded that a lognormal distribution is sufficient for assigning uncertainties to these data.

Both the CTD and the XCTD estimates in Fig. 4 show values of similar order of magnitude to previous finescale estimates (Naveira Garabato et al. 2004; Thompson et al. 2007). For example, the magnitude and vertical structure of the CTD estimates for the southeastern Pacific stations are consistent with the estimates made by Sloyan et al. (2010) in the southeastern Pacific during austral winter of 2005 and austral summer of 2006, with κ values being highest below the mixed layer and decaying with depth.

The XCTD Thorpe scale κ estimates in Figs. 4a,b are inconsistent with the microstructure estimates and with previous observations from tracer diffusion (Ledwell et al. 2011) and LADCP (Naveira Garabato et al. 2004). The XCTD estimates are approximately two orders of magnitude larger than the microstructure estimates, and do not reproduce the vertical structure that is seen in the microstructure κ. The CTD Thorpe scale estimates in the southeastern Pacific (Fig. 4a) show similar inconsistencies with microstructure above 600 m, but below that depth they become more consistent with the microstructure estimates. In Drake Passage, the magnitudes of the CTD κ estimates are consistent with the microstructure estimates for all depth bins.

As the noise estimates discussed in section 2 show, instrument noise in our data can produce false overturns of approximately 20 m for the XCTD and approximately 4 m for the CTD. Noise has a nonlinear effect on the Thorpe-scale calculation. Both positive and negative noise-related density spikes imply density displacements, which augment L_T, and regardless of sign, noise can extend the overturn length. In general, we find that this effect is more pronounced for the XCTD than for the CTD data. Figure 5a shows that even after filtering, the typical XCTD potential density profile shows larger and more frequent density variations over a given depth range compared with a CTD profile sampled at the same location. The effect of these variations on overturn size can be seen in the probability density functions (PDFs) of Drake Passage and southeastern Pacific overturn sizes for XCTDs and CTDs (Fig. 6). The PDFs were calculated using overturns that were prevalidated by passing all validation criteria except for the minimum overturn test. In Drake Passage, the PDF for XCTD overturns (Fig. 6b) peaks at 25–26 m, while the PDF for CTD overturns (Fig. 6d) peaks at 9–10 m. The peaks for both instruments occur within 5 m of minimum resolvable overturn size. However, as discussed in section 2, the density uncertainty in the XCTD data corresponds to a depth change of 5–7 m, while the density uncertainty in the CTD data corresponds to a depth change of 0.5–1.5 m. Thus, the XCTD data in Drake Passage are more likely to have noise-generated false overturns. In comparison, the PDFs in the southeastern Pacific for both the CTD and the XCTD (Figs. 6a,c) peak within 1.5 m of the minimum overturn size, indicating that estimates by both instruments are likely to be contaminated by false overturns.

The differences in the PDFs shown in Fig. 6 and the high values of XCTD estimates compared with CTD and microstructure raise the possibility that not enough false overturns are being discarded, and that the estimates could be improved by increasing the minimum overturn size for XCTDs above 20 m. However, the XCTD estimates would not agree with the microstructure estimates within error bars unless the minimum overturn size were increased to approximately 90 m. With that criterion, over 98% of all overturns would be discarded, and the κ estimates become uniform for all bins, indicating that too many real overturns would have to be discarded to produce a meaningful estimate. The persistence of overly large estimates even with a high minimum overturn criterion suggests that the instrument noise in XCTD data either produces enough false large overturns or increases the apparent size of real overturns to cause consistent overestimation of κ. Therefore, using XCTD data in conjunction with the Thorpe-scale method can provide an upper bound on mixing.

The accuracy of the Thorpe-scale estimates is dependent on the instrument noise, the local stratification,
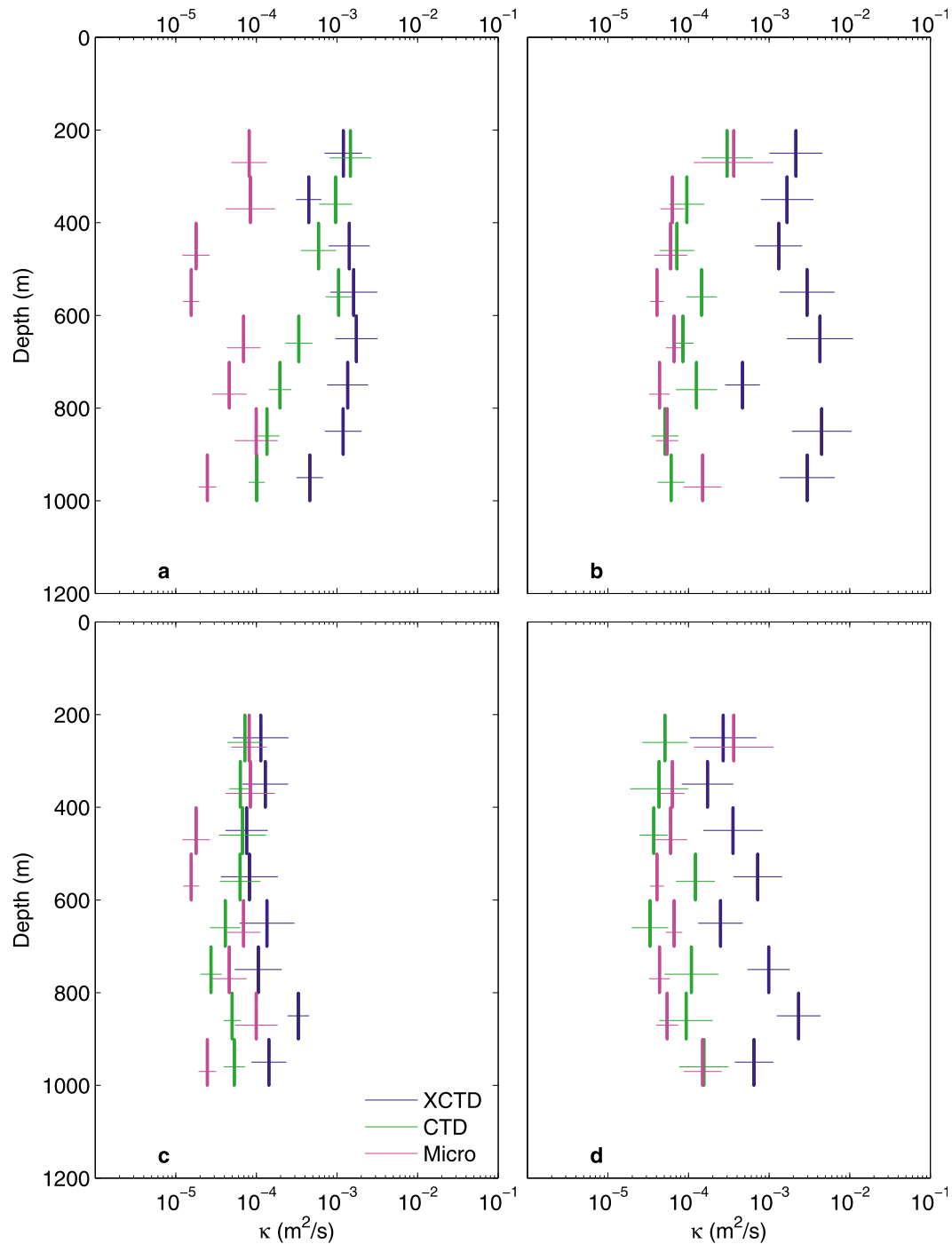
FIG. 4. (top) Thorpe-scale and (bottom) strain estimates of κ computed from CTD and XCTD data sampled during the DIMES survey in January and February 2010 in (a),(c) southeastern Pacific and (b),(d) Drake Passage. Estimates derived from microstructure measurements of velocity shear are also plotted for comparison purposes. Results shown here are based on stations for which all three instruments were available (red stars in Fig. 1). Error bars represent one standard error based on the standard deviation of $\log_{10}(\kappa)$.
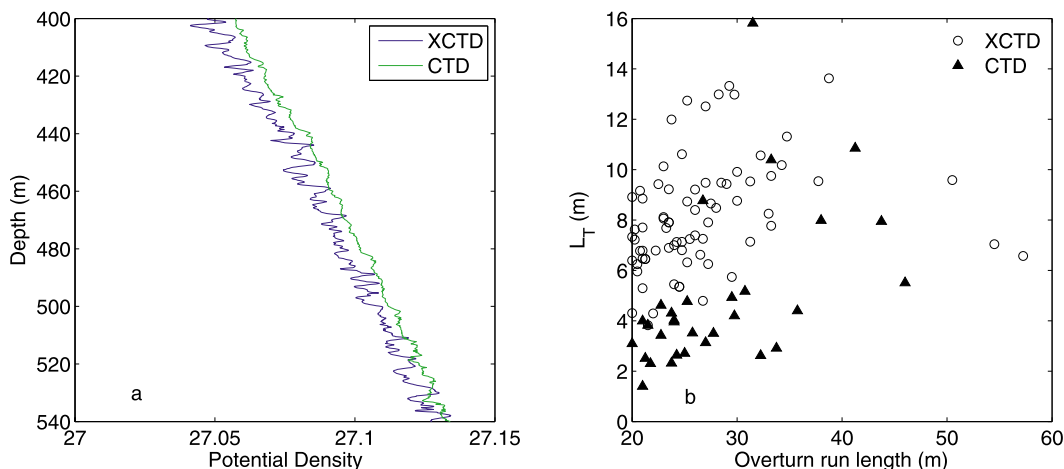
FIG. 5. Comparison of (a) potential density of a representative filtered CTD and XCD profile sampled at the same location and (b) Thorpe scales vs overturn run length for CTD and XCTD data.

and the typical size of true density displacements relative to background noise. If the difference between the minimum resolvable overturn size and the peak of the PDF of overturn sizes is smaller than the uncertainty caused by instrument noise, then Thorpe-scale estimates of diffusivity are unlikely to be robust.

If the percentage of large displacements were consistent between the southeastern Pacific and Drake Passage, then Thorpe scales might be expected to yield useful information about the spatial patterns of κ. However, our results show that this is not the case for the low-stratification conditions found in the Antarctic
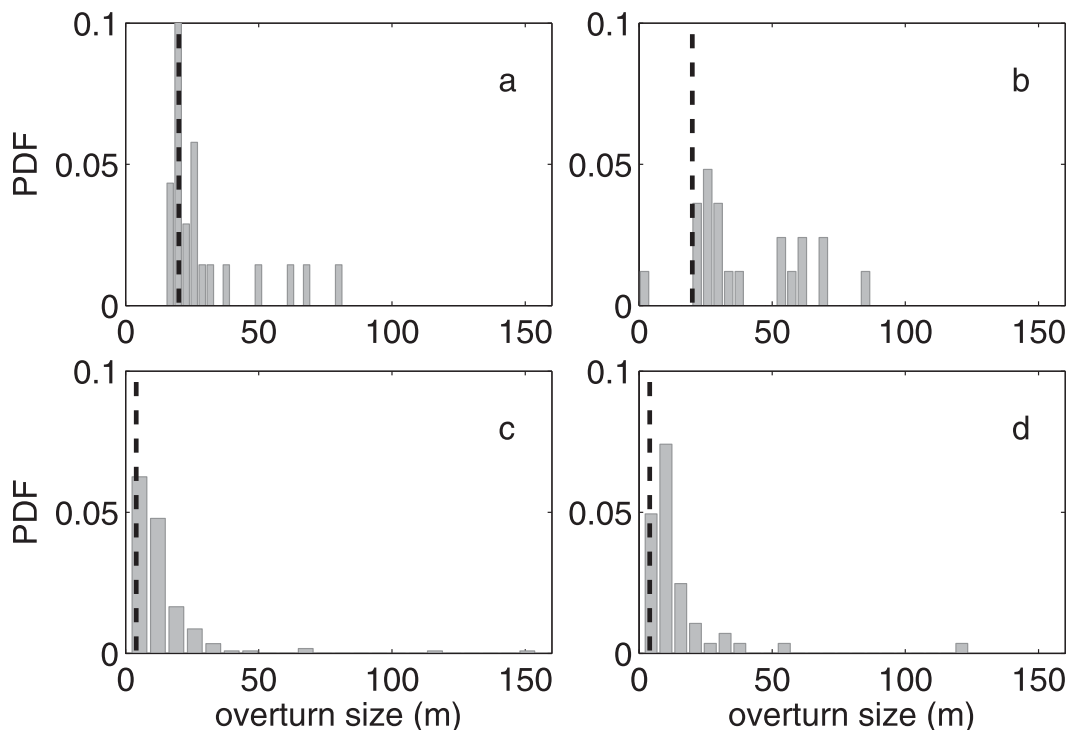

FIG. 6. PDF of the size of prevalidated overturns detected in (a),(c) the southeastern Pacific and (b),(d) Drake Passage by (top) XCTD and (bottom) CTD. Black dashed lines indicate the minimum resolvable overturn size for each instrument. Overturns are considered prevalidated if they have passed all overturn validation criteria other than the minimum size test. The number of validated overturns in Drake Passage is 21 for the XCTD and 51 for the CTD, while the number of overturns in the southeastern Pacific is 51 for the XCTD and 166 for the CTD.

Circumpolar Current (ACC). In regions such as the Admiralty Inlet at the entrance to Puget Sound (Seim and Gregg 1994) or Kaena Ridge near Hawaii (Klymak et al. 2008), where stratification is one to two orders of magnitude higher than in the DIMES region, the magnitude of noise-generated overturns is correspondingly smaller, and Thorpe-scale estimates match more closely with the microstructure.

XCTD Thorpe scales produce higher values of κ than the CTD estimates, with Drake Passage values up to two orders of magnitude larger (Fig. 4). In addition the XCTD estimates have larger error bars. A comparison of CTD and XCTD salinity spectra (Fig. 2c) shows different spectral slopes in the 10^{-1} to 10^0 cpm frequency range, even after careful processing to minimize noise, as discussed in section 2. The differences between the CTD and XCTD spectra are greater for salinity than for temperature, indicating that it is the combination of salinity spiking and the larger-magnitude noise in the raw conductivity data for the XCTD that causes the density difference between the two instruments, even after extensive filtering. Additional low-pass filtering at lower wavenumbers would further reduce the noise, but at the cost of reducing the accuracy of the resulting estimates, because filtering would also increase the minimum resolvable overturn size and filter out parts of the true turbulence signal along with noise.

b. Vertical strain method

Estimates of κ computed using the vertical strain analysis described in section 2 are shown in Figs. 4c,d. Again, microstructure-based diffusivities (magenta) are indicated for comparison. Mean diffusivities for the strain analysis are determined in the same way as for Thorpe scales, by averaging all estimates within a depth bin, and error bars are again assigned assuming a lognormal distribution.

Compared with the Thorpe-scale method, the strain method produces significantly smaller differences between the XCTD and CTD estimates, and between finescale instruments and microstructure. The XCTD estimates show a wider range of values and larger error bars than the CTD estimates, and XCTD estimates consistently exceed CTD and microstructure estimates, particularly in Drake Passage below 600 m. The differences in the XCTD and CTD estimates reflect the spectral differences between the two instruments, as shown in Fig. 2c.

c. Diffusivity in Drake Passage versus the southeastern Pacific

At the most basic level, a successful finescale parameterization should capture the increase in vertical diffusivity between the southeastern Pacific and the Drake Passage. In Fig. 7, magenta lines indicate the ratio of microstructure κ in Drake Passage to microstructure κ over the abyssal plain. Uncertainties are determined by propagating the errors from the averaged κs shown in Fig. 4. Half the bins show ratios greater than one, which is generally consistent with tracer diffusivity differences inferred in the same region (Ledwell et al. 2011). The remaining bins show no significant variation between the two regions.

For Thorpe scales, Fig. 7a compares the XCTD and CTD diffusivity ratios against the equivalent microstructure ratios at stations where data from all instruments were available. The CTD Thorpe-scale estimates (green) indicate a ratio that is consistently less than one. This appears to be primarily due to the relatively high CTD estimates in the southeastern Pacific (Fig. 4a), as compared with the corresponding estimates in Drake Passage, which are close to the microstructure estimates. The XCTD estimates (blue) for the southeastern Pacific show no significant spatial variation. Both the CTD and XCTD ratios are inconsistent with the microstructure ratios and with previous observations (Ledwell et al. 2011; Naveira Garabato et al. 2004; St. Laurent et al. 2012; Sheen et al. 2013), which indicate that diffusivities in Drake Passage are elevated compared with values from the abyssal plain. Thus, in this region, the Thorpe-scale method provides no formal means to distinguish the high-mixing and low-mixing regimes, despite the good agreement between CTD and microstructure in Drake Passage.

Strain method ratios are shown in Fig. 7b. The XCTD ratios lie between 10^0 and 10^1, with values at some depths that are substantially larger than the microstructure ratios. The CTD ratios are consistently smaller than the XCTD ratios, with ratios in the 200–300- and 400–500-m bins being smaller than the corresponding microstructure ratios by at least one standard error. Neither the XCTD nor the CTD reproduces the vertical structure of the microstructure ratios. When viewed over the entire water column, however, the strain method does appear to differentiate regions of high and low mixing.

d. Quantifying diffusivity

A second test of a successful finescale parameterization is whether it provides reasonable quantitative estimates of the vertical diffusivity. Studies in Kaena Ridge, Hawaii (Klymak et al. 2008), and the Romanche Fracture Zone near the Brazil Basin (Ferron et al. 1998) show good agreement between finescale and microstructure estimates. However, Waterman et al.'s (2013) ratios of microstructure and shear/strain finescale diffusivities computed near the Kerguelen Plateau indicate that in regions of low stratification, shear/strain estimates over
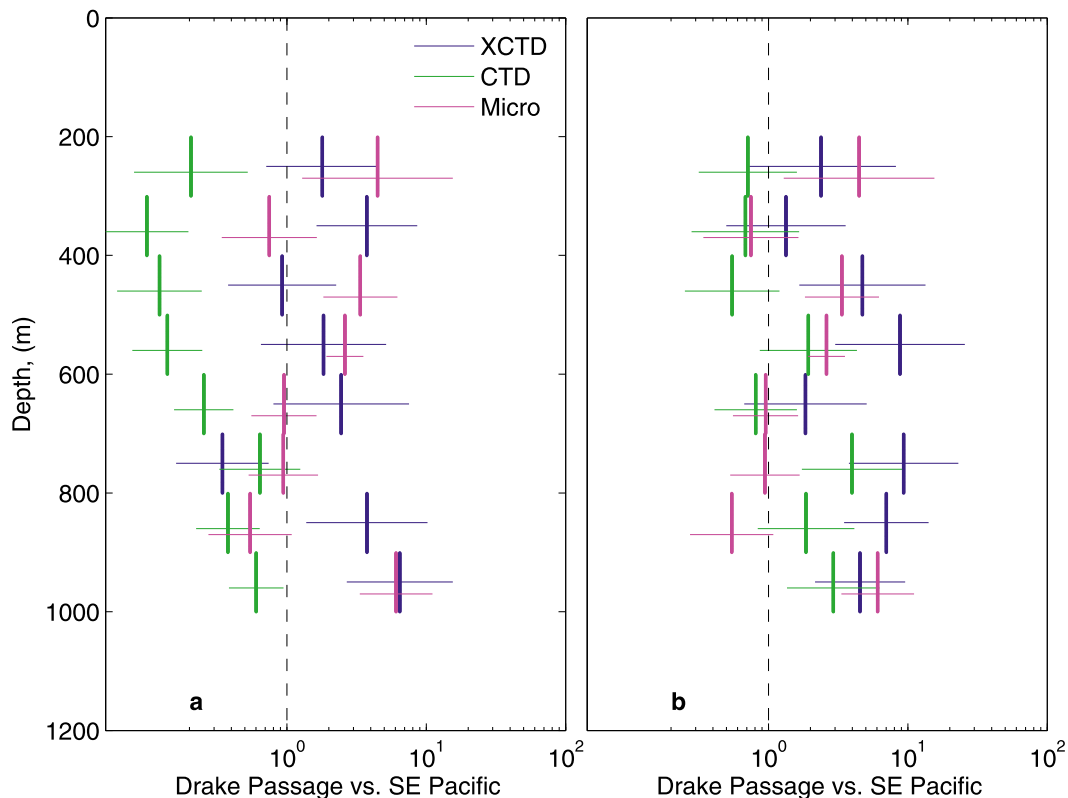
FIG. 7. The ratios of (a) Thorpe and (b) strain estimates of κ in Drake Passage to the estimates in the southeastern Pacific. Estimates derived from microstructure measurements of velocity shear are also plotted for comparison purposes.

rough topography in the top 1000 m of the ocean may only be expected to provide order-of-magnitude agreement with microstructure diffusivities, and we probably cannot expect them to agree by better than a factor of 2 or 3. While the lack of shear/strain measurements in our dataset makes it impractical to directly compare our results with those of Waterman et al. (2013), the relationship between our finescale and microstructure diffusivities allows us to compare the performance of density-based estimates of κ with the shear/strain estimates in the low-stratification environment of the Southern Ocean.

Figure 8 shows ratios of finescale diffusivity to microstructure diffusivity for the two regions. For both the Thorpe-scale (Figs. 8a,b) and strain (Figs. 8c,d) estimates, the XCTD diffusivity exceeds the microstructure diffusivity (blue). For the Thorpe-scale approach, differences can be as much as two orders of magnitude, while the strain diffusivities provide a better match but can still exceed the microstructure by an order of magnitude or more at some depths. The Thorpe-scale overestimates are consistent with indications that instrument noise in XCTD measurements can lead to inflated estimates of diffusivity.

The CTD-derived finescale estimates provide a better quantitative match (green lines in Fig. 8), but can still differ from microstructure κ by an order of magnitude, particularly for the Thorpe-scale method in the low-diffusivity region of the southeastern Pacific (Fig. 8a). The best finescale/microstructure agreement appears to occur for the Thorpe-scale-based analysis of CTD data collected in Drake Passage, where microstructure measurements reflect the presence of enhanced mixing. However, the Thorpe-scale method's sensitivity to noise means that the method does not perform well in low-stratification regimes where real and noise-generated overturns are not easily distinguished. Instrument noise will always amplify Thorpe scales; therefore, the method will produce an upper bound on mixing.

For the strain method, CTD-derived κ usually agree with microstructure-derived κ within statistical uncertainty, though these statistical uncertainties can be large. The ratios of CTD strain estimates to microstructure estimates are within one order of magnitude for all depth bins except for the topmost bin in Drake Passage, suggesting that density-based strain estimates computed from CTD data perform similarly to shear/strain estimates despite the assumption of constant R_ω.
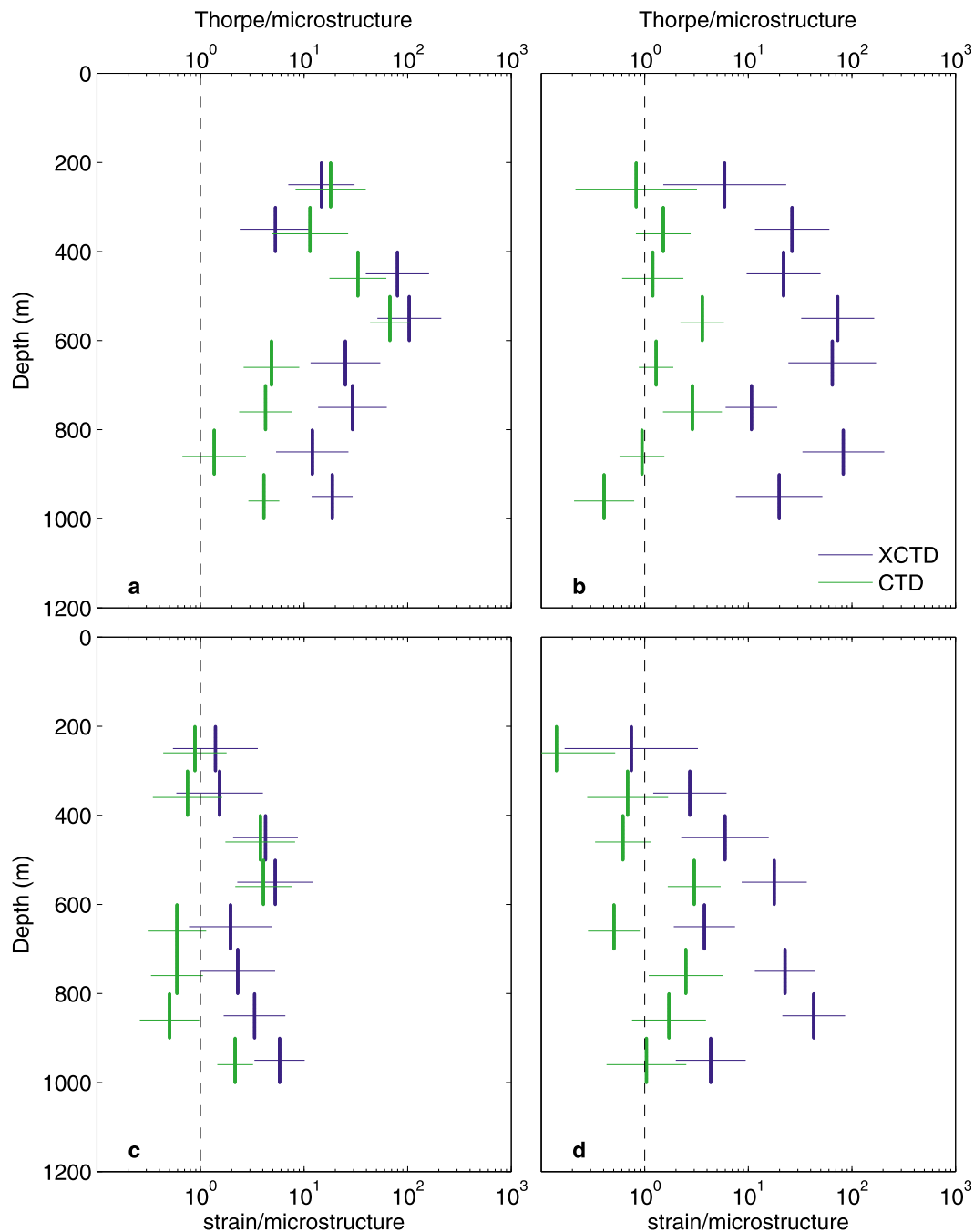
FIG. 8. The ratios of (top) Thorpe-scale and (bottom) strain estimates of κ to microstructure estimates for CTD and XCTD in (a),(c) southeastern Pacific and (b),(d) Drake Passage.

4. Summary

Finescale estimates of diapycnal diffusivities in the Southern Ocean were computed from CTD and XCTD data sampled during the DIMES survey in January and February of 2010. Both the Thorpe-scale and the vertical strain methods produced values of κ on the order of 10^{-4} to 10^{-3} m^2 s^{-1}. The finescale methods for the CTD and the XCTD tend to overestimate κ by at least an order of magnitude when compared with the microstructure, except in the top 500 m in Drake Passage, where the strain method for the CTD tends to underestimate κ when compared with the microstructure estimates.

A close examination of the noise characteristics of CTD and XCTD data indicates that once the data have been processed to minimize instrument noise, salinity spiking, and ship effects, the minimum size of resolvable density overturns for Thorpe scales is approximately 4 m for CTD data and 20 m for the XCTD. In our study regions, this leads to Thorpe-scale estimates exceeding the microstructure κ values by up to two orders of magnitude for XCTD data, while microstructure and CTD values match within an order of magnitude in Drake Passage. In high-stratification regions, where instrument noise of the same magnitude would produce smaller false overturns, Thorpe-scale analysis has the potential to produce more accurate estimates.

The uncertainty in κ estimates for the strain method is also considerable, with values often overestimated in the southeastern Pacific, although the CTD estimates showed improved agreement with microstructure, particularly in Drake Passage. Neither the XCTD nor the CTD precisely reproduce the differences in diffusivity that have been previously measured between Drake Passage and the low-mixing region in the eastern Pacific section of the survey (Ledwell et al. 2011; St. Laurent et al. 2012). However, the strain estimates provide a more consistent representation of the spatial variations, and the CTD yields more robust results with smaller statistical uncertainties than the XCTD.

Our analysis implies that CTD and XCTD measurements do not precisely replicate the microstructure estimates of small-scale mixing in the low-stratification regime characteristic of the Southern Ocean. However, the CTD performs significantly better than the XCTD for the Thorpe-scale method in Drake Passage and for the strain method in both Drake Passage and the southeastern Pacific. The performance difference between the two instruments is driven primarily by the greater magnitude noise in the XCTD data, which makes true density displacements indistinguishable from noise-generated displacements.

Low stratification in our study region magnifies the effects of noise by magnifying the displacements caused by noise-generated density spikes. The Thorpe-scale method has the potential to produce accurate estimates in regions where the stratification is high and mixing is characterized by large density overturns (Klymak et al. 2008; Ferron et al. 1998; Seim and Gregg 1994). In particular, ship motion effects can be minimized through the use of a stable platform (Klymak et al. 2008) or free-falling instruments that are less subject to background noise than the XCTD (Seim and Gregg 1994). A shear/strain approach based on a combination of CTD and LADCP data may offer further possibilities for minimizing discrepancies between microstructure and finescale diffusivity estimates.

REFERENCES

Bendat, J. S., and A. G. Piersol, 2000: *Random Data: Analysis and Measurement Procedures.* 3rd ed. John Wiley and Sons Ltd., 594 pp.

Crawford, W., 1986: A comparison of length scales and decay times of turbulence in stably stratified flows. *J. Phys. Oceanogr.,* **16,** 1847–1854.

Davis, R. E., 1996: Sampling turbulent dissipation. *J. Phys. Oceanogr.,* **26,** 341–358.

Dillon, T. M., 1982: Vertical overturns: A comparison of Thorpe and Ozmidov scales. *J. Geophys. Res.,* **87** (C12), 9601–9613.

Ferron, B., H. Mercier, K. Speer, A. Gargett, and K. Polzin, 1998: Mixing in the Romanche Fracture Zone. *J. Phys. Oceanogr.,* **28,** 1929–1945.

Galbraith, P. S., and D. E. Kelley, 1996: Identifying overturns in CTD profiles. *J. Atmos. Oceanic Technol.,* **13,** 688–702.

Gargett, A., and T. Garner, 2008: Determining Thorpe scales from ship-lowered CTD density profiles. *J. Atmos. Oceanic Technol.,* **25,** 1657–1670.

Garrett, C., and W. Munk, 1975: Space-time scales of internal waves: A progress report. *J. Geophys. Res.,* **80** (3), 291–297.

Gille, S. T., K. Speer, J. R. Ledwell, and A. C. Naveira Garabato, 2007: Mixing and stirring in the Southern Ocean. *Eos, Trans. Amer. Geophys. Union,* **88,** 382–383.

——, A. Lombrozo, J. Sprintall, G. Stephenson, and R. Scarlet, 2009: Anomalous spiking in spectra of XCTD temperature profiles. *J. Atmos. Oceanic Technol.,* **26,** 1157–1164.

——, and Coauthors, 2012: The diapycnal and isopycnal mixing experiment: A first assessment. *CLIVAR Exchanges,* No. 1, International CLIVAR Project Office, Southampton, United Kingdom, 46–48.

Gregg, M. C., 1987: Diapycnal mixing in the thermocline: A review. *J. Geophys. Res.,* **92** (C5), 5249–5286.

——, and E. Kunze, 1991: Shear and strain in Santa Monica Basin. *J. Geophys. Res.,* **96** (C9), 16 709–16 719.

Jochum, M., 2009: Impact of latitudinal variations in vertical diffusivity on climate simulations. *J. Geophys. Res.,* **114,** C01010, doi:10.1029/2008JC005030.

Johnson, G. C., J. M. Toole, and N. G. Larson, 2007: Sensor corrections for Sea-Bird SBE-41 CP and SBE-41 CTDs. *J. Atmos. Oceanic Technol.,* **24,** 1117–1130.

Klymak, J. M., R. Pinkel, and L. Rainville, 2008: Direct breaking of the internal tide near topography: Kaena Ridge, Hawaii. *J. Phys. Oceanogr.,* **38,** 380–399.

Kunze, E., 2003: Yes, we have no abyssal mixing. *Near-Boundary Processes and Their Parameterizations: Proc. 'Aha Huliko'a Hawaiian Winter Workshop,* Honolulu, HI, University of Hawai'i at Mānoa, 85–93.

——, E. Firing, J. M. Hummon, T. K. Chereskin, and A. Thurnherr, 2006: Global abyssal mixing inferred from lowered ADCP shear and CTD strain profiles. *J. Phys. Oceanogr., 36,* 1553–1576.

Ledwell, J. R., E. T. Montgomery, K. L. Polzin, L. C. St. Laurent, R. W. Schmitt, and J. M. Toole, 2000: Evidence for enhanced mixing over rough topography in the abyssal ocean. *Nature, 403,* 179–182.

——, L. C. St. Laurent, J. B. Girton, and J. M. Toole, 2011: Diapycnal mixing in the Antarctic Circumpolar Current. *J. Phys. Oceanogr., 41,* 4241–246.

MacKinnon, J. A., and Coauthors, 2010: Using global arrays to investigate internal-waves and mixing. *Proceedings of OceanObs'09: Sustained Ocean Observations and Information for Society,* J. Hall, D. E. Harrison, and D. Stammer, Eds., Vol. 2, ESA Publ. WPP-306, doi:10.5270/OceanObs09.cwp.58.

Martin, J. P., and D. L. Rudnick, 2007: Inferences and observations of turbulent dissipation and mixing in the upper ocean at the Hawaiian Ridge. *J. Phys. Oceanogr., 37,* 476–494.

Munk, W., and C. Wunsch, 1998: Abyssal recipes II: Energetics of tidal and wind mixing. *Deep-Sea Res. I, 45,* 1997–2010.

Naveira Garabato, A. C., K. L. Polzin, B. A. King, K. J. Heywood, and M. Visbeck, 2004: Widespread intense turbulent mixing in the Southern Ocean. *Science, 303,* 210–213.

Nikurashin, M., and S. Legg, 2011: A mechanism for local dissipation of internal tides generated at rough topography. *J. Phys. Oceanogr., 41,* 378–395.

Ozmidov, R. V., 1965: On the turbulent exchange in a stably stratified ocean. *Izv. Acad. Sci. USSR Atmos. Oceanic Phys., 1,* 861–871.

Palmer, M. D., A. C. Naveira Garabato, J. D. Stark, J. J. Hirschi, and J. Marotzke, 2007: The influence of diapycnal mixing on quasi-steady overturning states in the Indian Ocean. *J. Phys. Oceanogr., 37,* 2290–2304.

Polzin, K. L., J. M. Toole, and R. W. Schmitt, 1995: Finescale parameterizations of turbulent dissipation. *J. Phys. Oceanogr., 25,* 306–328.

Roemmich, D., and Coauthors, 2009: The Argo program: Observing the global ocean with profiling floats. *Oceanography, 22,* 24–33.

Seim, H. E., and M. C. Gregg, 1994: Detailed observations of a naturally occurring shear instability. *J. Geophys. Res., 99* (C5), 10 049–10 073.

Sheen, K. L., and Coauthors, 2013: Rates and mechanisms of turbulent dissipation and mixing in the Southern Ocean: Results from the Diapycnal and Isopycnal Mixing Experiment in the Southern Ocean (DIMES). *J. Geophys. Res. Oceans, 118,* 2774–2792, doi:10.1002/jgrc.20217.

Simmons, H. L., S. R. Jayne, L. C. St Laurent, and A. J. Weaver, 2004: Tidally driven mixing in a numerical model of the ocean general circulation. *Ocean Modell., 6,* 245–263, doi:10.1016/S1463-5003(03)00011-8.

Sloyan, B. M., 2005: Spatial variability of mixing in the Southern Ocean. *Geophys. Res. Lett., 32,* L18603, doi:10.1029/2005GL023568.

——, L. D. Talley, T. K. Chereskin, R. Fine, and J. Holte, 2010: Antarctic Intermediate Water and Subantarctic Mode Water formation in the southeast Pacific: The role of turbulent mixing. *J. Phys. Oceanogr., 40,* 1558–1574.

St. Laurent, L. C., A. C. Naveira Garabato, J. R. Ledwell, A. M. Thurnherr, and J. M. Toole, 2012: Turbulence and diapycnal mixing in Drake Passage. *J. Phys. Oceanogr., 42,* 2143–2152.

Thompson, A. F., S. T. Gille, J. A. MacKinnon, and J. Sprintall, 2007: Spatial and temporal patterns of small-scale mixing in Drake Passage. *J. Phys. Oceanogr., 37,* 572–592.

Thorpe, S. A., 1977: Turbulence and mixing in a Scottish loch. *Philos. Trans. Roy. Soc. London, 286A,* 125–181.

Toole, J. M., K. L. Polzin, and R. W. Schmitt, 1994: Estimates of diapycnal mixing in the abyssal ocean. *Science, 264,* 1120–1123.

Uchida, H., K. Shimada, and T. Kawano, 2011: A method for data processing to obtain high-quality XCTD data. *J. Atmos. Oceanic Technol., 28,* 816–826.

Waterman, S., A. C. Naveira Garabato, and K. L. Polzin, 2013: Internal waves and turbulence in the Antarctic Circumpolar Current. *J. Phys. Oceanogr., 43,* 259–282.

Whalen, C. B., L. D. Talley, and J. A. MacKinnon, 2012: Spatial and temporal variability of global ocean mixing inferred from Argo profiles. *Geophys. Res. Lett., 39,* L18612, doi:10.1029/2012GL053196.

Wijesekera, H., L. Padman, T. Dillon, M. Levine, C. Paulson, and R. Pinkel, 1993: The application of internal-wave dissipation models to a region of strong mixing. *J. Phys. Oceanogr., 23,* 269–286.

Wu, L., Z. Xing, S. Riser, and M. Visbeck, 2011: Seasonal and spatial variations of Southern Ocean diapycnal mixing from Argo profiling floats. *Nat. Geosci., 4,* 363–366.